Journal of Fluids and Structures (2002) **16**(4), 561–580
doi:10.1006/jfls.2001.0430, available online at http://www.idealibrary.com on IDEAL®

HYDROELASTIC VIBRATION OF A CIRCULAR CONTAINER BOTTOM PLATE USING THE GALERKIN METHOD

Y. K. CHEUNG

Department of Civil Engineering, The University of Hong Kong, Hong Kong

AND

D. ZHOU

Department of Mechanics and Engineering Science, Nanjing University of Science and Technology, Nanjing 210014, *People's Republic of China*

(Received 10 January 2000, and in final form 23 August 2001)

The free vibration of a flexible thin plate placed into a circular hole and elastically connected to the rigid bottom slab of a circular cylindrical container filled with fluid having a free surface is studied. The liquid is assumed to be incompressible, inviscid and irrotational. The effect of the free surface wave is also taken into account in the analysis. First of all, the exact expression of velocity potential of the liquid movement is derived by a combination of the superposition method and the method of separation of variables. With the help of the Fourier–Bessel series expansion, part of the unknown coefficients in the solution is determined by the consistency condition between the liquid movement and the plate vibration, in the form of integrals associated with the dynamic deflection of the plate. Then, the Galerkin method is applied to derive the eigenfrequency equation of the fluid–plate interaction. Finally, the effects of various parameters and the free surface wave on eigenfrequencies of the fluid–plate system are discussed. As a consequence, the accuracy of the nondimensional added virtual mass incremental (NAVMI) factor solution has also been evaluated by comparing with the more accurate Galerkin solution. It is shown that the proposed method is also applicable to the vibration analysis of circular plates in contact with an infinite liquid by only taking a finite but larger size of liquid to replace the infinite liquid in the computation.

1. INTRODUCTION

IT IS OF GREAT IMPORTANCE to understand the free vibration characteristics of fluid–plate interaction so that, for example, the propellant in space vehicles can be free from resonance, large-capacity oil containers in petrochemical industry can survive earthquakes, and ships and submarines can avoid or be subjected to reduced localized vibrations. It is generally accepted that a plate in contact with fluid behaves differently from the same plate in air and that the eigenfrequencies of the plate in contact with liquid are always lower than those in air.

Numerous investigations, both theoretical and experimental, can be found on circular cylindrical containers filled with liquids, because of their wide applicability in branches of engineering. Bhuta & Koval (1964*a*, *b*) studied the coupled vibration of liquid in a rigid circular cylindrical container with a flexible bottom which is treated as a flexible membrane or an elastic plate. The same problem was investigated by Tong (1967). Tsui & Small (1968)

0889–9746/02/040561 + 20 $35.00/0

investigated the coupled oscillation of liquid in an annular circular cylindrical container with a flexible bottom. Bauer *et al.* (1971) examined the nonlinear longitudinal oscillation of liquid in a circular cylindrical container with an elastic bottom. Furthermore, Bauer (1981, 1995) investigated the hydroelastic vibration of liquid in a rectangular container and a circular cylindrical container, respectively, of which the free liquid surface is covered by a flexible membrane or an elastic plate. Recently, Chiba (1993, 1994) studied the hydroelastic vibration of the flexural bottom in a circular cylindrical container under the consideration of the effect of in-plane force in the plate due to the static liquid pressure. Amabili (1997) and Amabili & Dalpiaz (1998) studied the bulging modes of an elastic bottom in circular and annular cylindrical containers partially filled with liquid by using the Ritz method. Cheung & Zhou (2000) and Zhou & Cheung (2000) analysed the hydroelastic vibration of a rectangular container bottom plate and a vertical rectangular plate, respectively, in contact with water on one side. Moreover, some investigators (Amabili 1996; Amabili & Kwak 1996; Espinosa & Gallego-Juarez 1984; Kwak 1991, 1997) studied the hydroelastic vibration of circular plates in contact with an infinite liquid. Taking into account the effect of free surface waves, Amabili & Kwak (1999) and Amabili *et al.* (1998) examined the vibration of circular plates on a free fluid surface and cylindrical tanks with flexible bottom, respectively. The present study can be considered as a general case of the elastic bottom in a rigid cylindrical container partially filled with liquid, i.e., a concentric circular part of the bottom is elastic, but the remaining parts are rigid. Moreover, the hydroelastic vibration of circular plates in contact with an infinite liquid can also be included in the present study by replacing the infinite liquid domain with a finite but larger-size liquid domain in the computation. Comparisons with available results show that this approximate approach has quite high accuracy (Amabili & Kwak 1996; Amabili 1996).

In this paper, attention is mainly focused on the bulging modes of the circular plate in contact with liquid, undergoing only small-amplitude oscillation. However, the sloshing modes are also included in the present analysis. Numerical results show that the effect of free-surface waves on the bulging modes of the bottom plate is not significant, unless the plate is extremely flexible. This phenomenon has also been observed experimentally (Amabili & Dalpiaz 1998) and in other theoretical studies (Amabili *et al.* 1998).

In the present study, the method of separation of variables is applied to obtain the solution of the velocity potential of the liquid and the Galerkin method is applied to derive the eigenfrequency equation of the liquid–plate system. The convergence study demonstrates high accuracy and small computational cost of the present approach. The NAVMI factor solution, of which the basic concept has been developed by Lamb (1921), is also obtained and compared with the more accurate Galerkin solution. Finally, some valuable results are presented, which can serve as a benchmark for further research on the aforementioned problem.

2. MOTION OF LIQUID

Consider an elastic circular plate placed into a hole of the rigid bottom slab of a circular cylindrical container partially filled with an inviscid, incompressible and irrotational liquid, as shown in Figure 1. The plate is thin, concentric with the rigid bottom slab, and made of linearly elastic, homogeneous and isotropic material. The effects of shear deflection and rotary inertia are neglected in the present analysis. The radii of the container and the circular plate are R_0 and R_1, respectively, the thickness of the plate is h and the depth of the liquid is H. The densities of the plate and the liquid are defined by ρ_p and ρ_l, respectively. The liquid has a free surface orthogonal to the axis of the container. Free-surface waves are considered in the present analysis, and a linear theory of liquid movement is adopted from

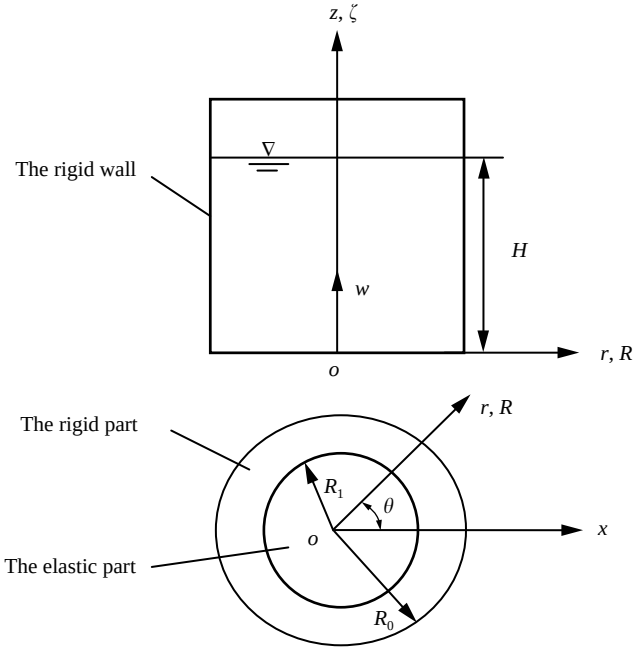

Figure 1. The geometry of a circular cylinder container with an elastic circular plate connected to the rigid bottom slab.

the small-amplitude oscillation of the liquid. The cylindrical coordinates are used to describe the movement of the liquid and the vibration of the plate, with the origin located at the centre of the bottom of the container. According to the above assumptions, the velocity potential of liquid movement should satisfy the Laplace equation,

$$\nabla^2\phi = \frac{\partial^2\phi}{\partial r^2} + \frac{1}{r}\frac{\partial\phi}{\partial r} + \frac{1}{r^2}\frac{\partial^2\phi}{\partial\theta^2} + \frac{\partial^2\phi}{\partial z^2} = 0, \tag{1}$$

in which the relations between ϕ and component velocities of the liquid are: $v_r = -\partial\phi/\partial r$, $v_\theta = -1/r\,\partial\phi/\partial\theta$, $v_z = -\partial\phi/\partial z$. The impermeability condition of vertical rigid wall is

$$\frac{\partial\phi}{\partial r} = 0, \quad r = R_0, \tag{2}$$

and ϕ should be finite at $r = 0$:

$$\phi = \text{finite value}, \quad r = 0. \tag{3}$$

It is obvious that ϕ should be 2π-periodic along the circumference, i.e.,

$$\phi(\theta + 2\pi) = \phi(\theta), \tag{4}$$

and the vibration of the liquid–plate system can be distinctly classified into symmetric modes and antisymmetric modes about the $\theta = 0$ axis. Without loss of generality, in the present analysis we shall only study the symmetric modes (antisymmetric modes can also be studied by the same procedure), i.e.,

$$\frac{\partial\phi}{\partial\theta} = 0, \quad \theta = 0. \tag{5}$$

Taking the effect of the surface wave into account, the free liquid surface equation is

$$\frac{\partial \phi}{\partial z} + \frac{1}{g}\frac{\partial^2 \phi}{\partial t^2} = 0, \quad z = H. \tag{6}$$

Considering that a concentric circular part of the bottom is elastic and the others are rigid, the consistency condition of the liquid movement and the plate vibration is

$$-\left.\frac{\partial \phi}{\partial z}\right|_{z=0} = \begin{cases} 0, & R_1 \le r \le R_0, \\ \dfrac{\partial w}{\partial t}, & 0 \le r < R_1, \end{cases} \tag{7}$$

in which w is the dynamic deflection of the plate and t denotes the time.

Applying the superposition method to solve the velocity potential, one can assume that

$$\phi = \bar{\phi} + \tilde{\phi}, \tag{8}$$

where $\bar{\phi}$ should satisfy such a free-surface condition that the effect of the free-surface wave is neglected:

$$\bar{\phi} = 0, \quad z = H, \tag{9}$$

while $\tilde{\phi}$ should satisfy the rigid-bottom condition

$$\frac{\partial \tilde{\phi}}{\partial z} = 0, \quad z = 0. \tag{10}$$

Inserting equation (8) into equations (6) and (7) and considering equations (9) and (10), we obtain

$$\frac{\partial \bar{\phi}}{\partial z} + \frac{\partial \tilde{\phi}}{\partial z} + \frac{1}{g}\frac{\partial^2 \tilde{\phi}}{\partial t^2} = 0, \quad z = H. \tag{11}$$

$$-\left.\frac{\partial \bar{\phi}}{\partial z}\right|_{z=0} = \begin{cases} 0, & R_1 \le r \le R_0, \\ \dfrac{\partial w}{\partial t}, & 0 \le r < R_1, \end{cases} \tag{12}$$

The first boundary condition and the equations of motion will be solved by the Galerkin method.

Introducing the nondimensional coordinates and parameters

$$R = r/R_0, \quad \zeta = z/H, \quad \alpha = R_1/R_0, \quad \beta = H/R_0 \tag{13}$$

and applying the method of separation of variables to equation (1), the solution of the liquid velocity potential can be given, after considering the boundary conditions (2)–(5) and (9)–(12), as follows:

$$\bar{\phi} = \mathrm{i}\omega H \mathrm{e}^{-\mathrm{i}\omega t} \sum_{n=0}^{\infty} \bar{\phi}_n(R, \zeta) \cos(n\theta), \tag{14}$$

$$\tilde{\phi} = \mathrm{i}\omega H \mathrm{e}^{-\mathrm{i}\omega t} \sum_{n=0}^{\infty} \tilde{\phi}_n(R, \zeta) \cos(n\theta), \tag{15}$$

where ω denotes the radian eigenfrequency of liquid–plate interaction, $\mathrm{i} = \sqrt{-1}$ and

$$\bar{\phi}_n(R, \zeta) = \sum_{m=1}^{\infty} A_{mn}\, \mathrm{J}_n(\varepsilon_{mn} R)\left[\cosh(\varepsilon_{mn}\beta\zeta) - \frac{\sinh(\varepsilon_{mn}\beta\zeta)}{\tanh(\varepsilon_{mn}\beta)}\right], \tag{16}$$

$$\tilde{\phi}_n(R, \zeta) = \sum_{j=1}^{\infty} D_{jn}\, \mathrm{J}_n(\varepsilon_{jn} R)\cosh(\varepsilon_{jn}\beta\zeta), \tag{17}$$

for $n \geq 1$, and

$$\bar{\phi}_0(R, \zeta) = A_{00}(1 - \zeta) + \sum_{m=1}^{\infty} A_{m0}\, \mathrm{J}_0(\varepsilon_{m0} R)\left[\cosh(\varepsilon_{m0}\beta\zeta) - \frac{\sinh(\varepsilon_{m0}\beta\zeta)}{\tanh(\varepsilon_{m0}\beta)}\right], \tag{18}$$

$$\tilde{\phi}_0(R, \zeta) = \mathrm{D}_{00} + \sum_{j=1}^{\infty} D_{j0}\, \mathrm{J}_0(\varepsilon_{j0} R)\cosh(\varepsilon_{j0}\beta\zeta). \tag{19}$$

In the above analysis, A_{mn} and D_{jn} ($m = n = j = 0$ and $m, n = 1, 2, \ldots$) are the unknown constants. ε_{mn} ($m = 1, 2, 3, \ldots, n = 0, 1, 2, \ldots$) are the roots of the derivative of Bessel function of the first kind of order n, i.e. (McLachlan 1961)

$$\mathrm{J}_n'(\varepsilon_{mn}) = 0, \quad m = 1, 2, 3, \ldots, \quad n = 0, 1, 2, \ldots \tag{20}$$

here, $(\ )'$ denotes the derivative to the argument.

It is assumed that the dynamic deflection of the circular plate can be written as

$$w = \mathrm{e}^{-\mathrm{i}\omega t} \sum_{n=0}^{\infty} w_n(R)\cos(n\theta), \tag{21}$$

substituting equations (14) and (21) into equation (12) gives

$$\left.\frac{\partial \bar{\phi}_n(R, \zeta)}{\partial \zeta}\right|_{\zeta = 0} = \begin{cases} 0, & \alpha \leq R \leq 1, \\ w_n(R), & 0 \leq R < \alpha. \end{cases} \tag{22}$$

Substituting equations (16) and (18) sequentially into the above equation, then applying the Bessel–Fourier expansion to the two sides of the equation in the interval [0, 1], one has

$$A_{mn} = -\frac{\tanh(\varepsilon_{mn}\beta)}{\varepsilon_{mn}\beta C_{mn}}\, Q_{mn}, \quad m = 1, 2, 3, \ldots, \quad n = 0, 1, 2, \ldots, \tag{23}$$

$$A_{00} = -2Q_{00}, \tag{24}$$

in which

$$C_{mn} = \int_0^1 R[\mathrm{J}_n(\varepsilon_{mn} R)]^2\, \mathrm{d}R = \frac{\varepsilon_{mn}^2 - n^2}{2\varepsilon_{mn}^2}\,[\mathrm{J}_n(\varepsilon_{mn})]^2, \tag{25}$$

$$Q_{mn} = \int_0^{\alpha} R w_n(R)\mathrm{J}_n(\varepsilon_{mn} R)\, \mathrm{d}R, \tag{26}$$

$$Q_{00} = \int_0^{\alpha} R w_0(R)\, \mathrm{d}R. \tag{27}$$

3. EIGENFREQUENCY EQUATION

From the linearized Bernoulli equation in fluid mechanics (Morand and Ohayon 1995), the dynamic pressure distribution of the liquid p acting on the plate is

$$p = \rho_l \frac{\partial \phi}{\partial t}\bigg|_{\zeta=0} = \mathrm{e}^{-\mathrm{i}\omega t} \sum_{n=0}^{\infty} p_n(R)\cos(n\theta). \tag{28}$$

Substituting equations (8) and (14)–(19) into the above equation, one has

$$p_n(R) = \rho_l \omega^2 H \sum_{n=0}^{\infty} [\bar{\phi}_n(R,\zeta) + \tilde{\phi}_n(R,\zeta)]|_{\zeta=0}. \tag{29}$$

According to the vibration theory of thin plates (Leissa 1969), the governing differential equation of the plate under the pressure distribution p is

$$D\nabla^4 w + \rho_p h \frac{\partial^2 w}{\partial t^2} = -p, \tag{30}$$

where $D = Eh^3/[12(1-\nu^2)]$ is the flexural rigidity of the plate; ν and E are Poisson's ratio and Young's modulus, respectively. $\nabla^4 = (\nabla^2)^2$ is the double Laplace operator. Substituting equations (17) and (19) into the above equation, one has

$$D\nabla_n^4 w_n(R) - \rho_p h\omega^2 w_n(R) = -\omega^2 \rho_l H[\bar{\phi}_n(R,\zeta) + \tilde{\phi}_n(R,\zeta)]|_{\zeta=0}, \tag{31}$$

where $\nabla_n^4 = (\nabla_n^2)^2$; $\nabla_n^2 = \mathrm{d}^2/\mathrm{d}r^2 + (1/r)\mathrm{d}/\mathrm{d}r - n^2/r^2$. It is assumed that the solution of the above equation can be expressed in the form

$$w_n(R) = \sum_{i=1}^{\infty} B_{in} w_{in}\left(\frac{k_{in}}{\alpha} R\right), \tag{32}$$

where B_{in} $(i = 1, 2, 3, \ldots)$ are the unknown constants, and $w_{in}(k_{in}R/\alpha)$ $(i = 1, 2, 3, \ldots)$ are the modes of the solid circular plate in air (Leissa 1969),

$$w_{in}\left(\frac{k_{in}}{\alpha} R\right) = \mathrm{J}_n\left(\frac{k_{in}}{\alpha} R\right) + a_{in}\,\mathrm{I}_n\left(\frac{k_{in}}{\alpha} R\right), \tag{33}$$

where $\mathrm{I}_n(k_{in}R/\alpha)$ is the modified Bessel function of the first kind of order n, and the constants a_{in} and k_{in} are determined by the boundary conditions on the plate. For example, if the plate is with elastically rotational constraint and zero deflection along the edge, one has

$$a_{in} = -\frac{\mathrm{J}_n(k_{in})}{\mathrm{I}_n(k_{in})} \tag{34}$$

and k_{in} $(i = 1, 2, 3, \ldots)$ are the roots of the following eigenvalue equation:

$$\begin{aligned} &\mathrm{J}_{n+2}(k_{in}) + \mathrm{J}_{n-2}(k_{in}) - \frac{2}{k_{in}}(\nu + K_\psi)[\mathrm{J}_{n+1}(k_{in}) - \mathrm{J}_{n-1}(k_{in})] \\ &\quad - \left(2 + \frac{4\nu n^2}{k_{in}^2}\right)\mathrm{J}_n(k_{in}) + a_{in}\{\mathrm{I}_{n+2}(k_{in}) + \mathrm{I}_{n-2}(k_{in}) \\ &\quad + \frac{2}{k_{in}}(\nu + K_\psi)[\mathrm{I}_{n+1}(k_{in}) + \mathrm{I}_{n-1}(k_{in})] + \left(2 - \frac{4\nu n^2}{k_{in}^2}\right)\mathrm{I}_n(k_{in})\} = 0, \end{aligned} \tag{35}$$

where $K_\psi = k_\psi R_1/D$ is the nondimensional stiffness of the rotational constraint k_ψ.

Truncating i in equation (32) up to $I+1$ and m and j in equations (16)–(19) up to $M+1$ and $J+1$, respectively, the eigenfrequency equation of the liquid–plate interaction can be

obtained by using the Galerkin method (multiplying the two sides of equation (31) by $w_{in}R(k_{in}/\alpha)$ and integrating between 0 and α) as follows:

$$\left\{\begin{bmatrix} k_{n1}^4 & & & \\ & k_{n2}^4 & 0 & \\ & 0 & \ddots & \\ & & & k_{nI}^4 \end{bmatrix} - \lambda^2\left(\begin{bmatrix} 1 & & & \\ & 1 & 0 & \\ & 0 & \ddots & \\ & & & 1 \end{bmatrix} + \frac{\sigma}{\gamma}\begin{bmatrix} \bar{m}_{11}^n & \bar{m}_{12}^n & \dots & \bar{m}_{1I}^n \\ \bar{m}_{21}^n & \bar{m}_{22}^n & \dots & \bar{m}_{2I}^n \\ \vdots & \vdots & \ddots & \vdots \\ \bar{m}_{I1}^n & \bar{m}_{I2}^n & \dots & \bar{m}_{II}^n \end{bmatrix}\right)\right\}\begin{bmatrix} B_{1n} \\ B_{2n} \\ \dots \\ B_{In} \end{bmatrix}$$

$$+ \lambda^2\frac{\sigma}{\gamma}\begin{bmatrix} \tilde{m}_{11}^n & \tilde{m}_{12}^n & \dots & \tilde{m}_{1J}^n \\ \tilde{m}_{21}^n & \tilde{m}_{22}^n & \dots & \tilde{m}_{2J}^n \\ \vdots & \vdots & \ddots & \vdots \\ \tilde{m}_{I1}^n & \tilde{m}_{I2}^n & \dots & \tilde{m}_{IJ}^n \end{bmatrix}\begin{bmatrix} D_{1n} \\ D_{2n} \\ \vdots \\ D_{Jn} \end{bmatrix} = 0 \qquad \text{for } n > 0, \tag{36}$$

$$\left\{\begin{bmatrix} k_{01}^4 & & & \\ & k_{02}^4 & 0 & \\ & 0 & \ddots & \\ & & & k_{0I}^4 \end{bmatrix} - \lambda^2\left(\begin{bmatrix} 1 & & & \\ & 1 & 0 & \\ & 0 & \ddots & \\ & & & 1 \end{bmatrix} + \frac{\sigma}{\gamma}\begin{bmatrix} \bar{m}_{11}^0 & \bar{m}_{12}^0 & \dots & \bar{m}_{1I}^0 \\ \bar{m}_{21}^0 & \bar{m}_{22}^0 & \dots & \bar{m}_{2I}^0 \\ \vdots & \vdots & \ddots & \vdots \\ \bar{m}_{I1}^0 & \bar{m}_{I2}^0 & \dots & \bar{m}_{II}^0 \end{bmatrix}\right)\right\}\begin{bmatrix} B_{10} \\ B_{20} \\ \vdots \\ B_{I0} \end{bmatrix}$$

$$+ \lambda^2\frac{\sigma}{\gamma}\begin{bmatrix} \tilde{m}_{10}^0 & \tilde{m}_{11}^0 & \tilde{m}_{12}^0 & \dots & \tilde{m}_{1J}^0 \\ \tilde{m}_{20}^0 & \tilde{m}_{21}^0 & \tilde{m}_{22}^0 & \dots & \tilde{m}_{2J}^0 \\ \vdots & \vdots & \vdots & \ddots & \vdots \\ \tilde{m}_{I0}^0 & \tilde{m}_{I1}^0 & \tilde{m}_{I2}^0 & \dots & \tilde{m}_{IJ}^0 \end{bmatrix}\begin{bmatrix} D_{00} \\ D_{10} \\ D_{20} \\ \vdots \\ D_{J0} \end{bmatrix} = 0 \qquad \text{for } n = 0. \tag{37}$$

In the above two equations,

$$\lambda^2 = \frac{\rho_p h}{D}\omega^2 R_1^4, \qquad \sigma = \frac{\rho_l}{\rho_p}, \qquad \gamma = \frac{h}{R_1}, \tag{38}$$

$$\bar{m}_{ij}^n = \left(\sum_{m=1}^{\infty}\frac{\tanh(\varepsilon_{mn}\beta)}{\varepsilon_{mn}C_{\mathrm{mn}}}Q_{imn}\,Q_{jmn}\right)\Big/(\alpha^3 m_{ii}^n) \text{ for } n > 0, \tag{39}$$

$$\bar{m}_{ij}^0 = 2Q_i^0 Q_j^0 + \left(\sum_{m=1}^{\infty}\frac{\tanh(\varepsilon_{m0}\beta)}{\varepsilon_{m0}C_{m0}}Q_{\mathrm{im0}}Q_{jm0}\right)/(\alpha^3 m_{ii}^0), \tag{40}$$

$$\tilde{m}_{ij}^n = \beta Q_{ijn}/(\alpha^3 m_{ii}^n) \text{ for } j \neq n \neq 0, \tag{41}$$

$$\tilde{m}_{i0}^0 = \beta Q_i^0/(\alpha^3 m_{ii}^0) \tag{42}$$

and

$$Q_{imn} = \int_0^{\alpha} R w_{in}\left(\frac{k_{in}}{\alpha}R\right)\mathrm{J}_n(\varepsilon_{mn}R)\,\mathrm{d}R = \frac{\alpha^2}{k_{\mathrm{in}}^2 - (\varepsilon_{mn}\alpha)^2}\{k_{in}\,\mathrm{J}_n(\varepsilon_{mn}\alpha)\,\mathrm{J}_{n+1}(\varepsilon_{mn}\alpha)$$

$$- \varepsilon_{mn}\alpha\mathrm{J}_n(k_{in})\,\mathrm{J}_{n+1}(\varepsilon_{mn}\alpha)\} + a_{in}\frac{\alpha^2}{k_{in}^2 + (\varepsilon_{mn}\alpha)^2}\{k_{in}\,\mathrm{I}_n(\varepsilon_{mn}\alpha)\,\mathrm{J}_{\mathrm{n}+1}(\varepsilon_{mn}\alpha)$$

$$+ \varepsilon_{mn}\alpha\mathrm{J}_n(k_{in})\,\mathrm{I}_{n+1}(\varepsilon_{mn}\alpha)\}, \tag{43}$$

$$Q_i^0 = \alpha^2\int_0^1 R w_{i0}(k_{i0}R)\,\mathrm{d}R = \alpha^2 w_1(k_{i0})/k_{i0}, \tag{44}$$

$$m_{ii}^n = \int_0^1 R w_{in}(k_{in}R)^2 \, \mathrm{d}R = \frac{1}{2}\left\{ \dot{\mathrm{J}}_n^2(k_{in}) + \left(1 - \frac{n^2}{k_{in}^2}\right) \mathrm{J}_n^2(k_{in}) - a_{in}^2 \left[\dot{\mathrm{I}}_n^2(k_{in}) - \left(1 + \frac{n^2}{k_{in}^2}\right) \mathrm{I}_n^2(\mathrm{k}_{in}) \right] \right\}$$

$$+ \frac{a_{in}}{k_{in}} [\mathrm{J}_n(k_{in})\, \mathrm{I}_{n+1}(k_{in}) + \mathrm{I}_n(k_{in})\, \mathrm{J}_{n+1}(k_{in})]. \tag{45}$$

It should be mentioned that when deriving equations (36) and (37), the orthogonal relations among dry modes of the circular plate have been utilized.

Finally, equations (36) and (37) can be written in a compact form as

$$\{[K] - \lambda^2([I] + \mu[\bar{M}])\}\{B\} + \lambda^2 \mu[\tilde{M}]\{D\} = 0, \tag{46}$$

in which, $[I]$ is a unit diagonal matrix, $\mu = \sigma/\gamma$ and $[\bar{M}]$ are, respectively, referred to as the density–thickness correction factor and the nondimensional added virtual mass incremental (NAVMI) matrix (Kwak 1991).

It is obvious that equation (46) cannot be solved until $\{D\}$ is given. However, substituting equations (14)–(19) into sloshing equation (11) provides a set of additional Galerkin equations which can be written in a matrix form as

$$\left\{ \begin{bmatrix} \bar{v}_{11}^n & \bar{v}_{12}^n & \cdots & \bar{v}_{1I}^n \\ \bar{v}_{21}^n & \bar{v}_{22}^n & \cdots & \bar{v}_{2I}^n \\ \cdots & \cdots & \ddots & \cdots \\ \bar{v}_{J1}^n & \bar{v}_{J2}^n & \cdots & \bar{v}_{JI}^n \end{bmatrix} \begin{bmatrix} B_{1n} \\ B_{2n} \\ \vdots \\ B_{In} \end{bmatrix} + \left(\begin{bmatrix} \tilde{v}_{11}^n & & & \\ & \tilde{v}_{22}^n & 0 & \\ & 0 & \ddots & \\ & & & \tilde{v}_{JJ}^n \end{bmatrix} - \lambda^2 t \begin{bmatrix} s_{11}^n & & & \\ & s_{22}^n & 0 & \\ & 0 & \ddots & \\ & & & s_{JJ}^n \end{bmatrix} \right) \begin{bmatrix} D_{1n} \\ D_{2n} \\ \vdots \\ D_{Jn} \end{bmatrix} \right\} = 0 \quad \text{for} \quad n > 0 \tag{47}$$

$$\left\{ \begin{bmatrix} 2Q_1^0 & 2Q_2^0 & \cdots & 2Q_I^0 \\ \bar{v}_{11}^0 & \bar{v}_{12}^0 & \cdots & \bar{v}_{1I}^0 \\ \bar{v}_{21}^0 & \bar{v}_{22}^0 & \cdots & \bar{v}_{2I}^0 \\ \vdots & \vdots & \ddots & \vdots \\ \bar{v}_{J1}^0 & \bar{v}_{J2}^0 & \cdots & \bar{v}_{JI}^0 \end{bmatrix} \begin{bmatrix} B_{10} \\ B_{20} \\ \cdots \\ B_{I0} \end{bmatrix} + \left(\begin{bmatrix} 0 & & & \\ & \tilde{v}_{11}^0 & & 0 \\ & & \tilde{v}_{22}^0 & \\ & 0 & & \ddots \\ & & & \tilde{v}_{JJ}^0 \end{bmatrix} - \lambda^2 t \begin{bmatrix} -1 & & & \\ & s_{11}^0 & & 0 \\ & & s_{22}^0 & \\ & 0 & & \ddots \\ & & & s_{JJ}^0 \end{bmatrix} \right) \begin{bmatrix} D_{00} \\ D_{10} \\ \vdots \\ D_{J0} \end{bmatrix} \right\} = 0 \quad \text{for} \quad n = 0. \tag{48}$$

In the above two equations,

$$\bar{v}_{ij}^n = Q_{jin} [\tanh(\varepsilon_{in}\beta) \sinh(\varepsilon_{in}\beta) - \cosh(\varepsilon_{in}\beta)]/C_{in},$$

$$\tilde{v}_{jj}^n = \varepsilon_{jn}\beta \sinh(\varepsilon_{jn}\beta), \quad s_{jj}^n = \cosh(\varepsilon_{jn}\beta), \quad t = D/(g\rho_p R_1^3 h) \tag{49}$$

where t is called rigidity–gravity ratio of the plate.

Combining equation (46) with equations (47) and (48), one has the following eigenvalue equation:

$$\left\{\begin{bmatrix}[K] & [0]\\ [\bar{V}] & [\tilde{V}]\end{bmatrix} - \lambda^2\begin{bmatrix}[I]+\mu[\bar{M}] & -\mu[\bar{M}]\\ [0] & t[S]\end{bmatrix}\right\}\begin{bmatrix}\{B\}\\ \{D\}\end{bmatrix} = 0. \tag{50}$$

Using standard eigenvalue programs, the nondimensional frequency parameter λ and corresponding eigenvector $\{B\}$ and $\{D\}$ can be easily obtained from the above equation. And vibration modes are determined by back-substitution of the eigenvalues, one by one, in the usual manner. It should be mentioned that when the sloshing equations (47) and (48) are added to the eigenvalue problem, in general the matrices are no longer symmetrical. This could give complex eigenvalues. However, in a recent paper, Amabili (2000) has demonstrated the formulation of $[\bar{V}] = \mu[\bar{M}]^{\mathrm{T}}$. In such a case, equation (50) can be transformed into a Galerkin equation for symmetric matrices that give real eigenvalues; this shows that real eigenvalues are obtained also in this case.

From equation (50), coupled sloshing and bulging modes can be simultaneously obtained. It is clear that if free-surface waves are neglected, then the eigenfrequency equation above will degenerate into

$$\{[K] - \lambda^2([I] + \mu[\bar{M}])\}\{B\} = 0. \tag{51}$$

4. STUDY OF CONVERGENCE

In order to demonstrate the high accuracy and the small computational cost of the proposed method, a convergence study of eigenfrequencies is first carried out for a clamped circular bottom plate in contact with liquid when considering the effect of free-surface waves. Two different plate–container radius ratios are considered: $\alpha = 0{\cdot}2$ and $\alpha = 1$. The liquid–plate density ratio is taken as $\sigma = 0{\cdot}15$; depth–radius ratio of liquid $\beta = 1$; thickness–radius ratio of the plate $\gamma = 0{\cdot}05$; the rigidity–gravity ratio $t = 0{\cdot}1$; and Poisson·s ratio $\nu = 0{\cdot}3$. Table 1 gives the first five nondimensional frequency parameters λ_{in} $(i = 1, 2, 3, 4, 5)$, respectively, for $n = 0$ and 1 with respect to different number of terms of dry modes, steadily increasing from 1 to 8. From the table, it is seen that the eigenfrequencies converge quickly and monotonically from the above by increasing the number of terms of the dry modes. Both the accuracy and the speed of convergence are basically unaffected by the number of nodal diameters and the plate–container radius ratio. This will ensure a small-size eigenfrequency equation to be solved for all cases. In general, eight terms of the dry modes can give the first five eigenfrequencies with sufficiently satisfactory accuracy.

Table 2 gives the first five nondimensional frequency parameters λ_{in} $(i = 1, 2, 3, 4, 5)$, respectively, for $n = 0$ and 1 with respect to the number of terms of the series in equations (28) and (29). It was found that the number of terms needed in the summation series increases with a decrease of the plate–container radius ratio α.

5. SURFACE WAVE EFFECT

A close scrutiny of the literature on hydroelastic analysis of liquid–plate and/or liquid–shell interaction shows that two different mathematical models are frequently applied when the liquids have a free surface. One of them neglects the effect of free-surface waves; in such a case only the bulging modes of the plates/shells are dealt with. The other takes the effect of free-surface waves into account, in which case both the bulging modes of the plates/shells and the sloshing modes of the liquids are considered. Therefore, it is very important to justify whether the effect of free-surface waves can be neglected, and under what circumstances.

TABLE 1
Nondimensional eigenfrequencies of bulging modes of clamped circular plates in contact with liquid by using different numbers of terms of dry modes; $M = 40$ and $J = 5$

α	I	λ_{1n}	λ_{2n}	λ_{3n}	λ_{4n}	λ_{5n}
$n = 0$						
0·2	1	6·0407				
	2	6·0351	30·400			
	3	6·0346	30·366	74·643		
	4	6·0345	30·360	74·585	138·69	
	5	6·0345	30·359	74·572	138·61	222·53
	6	6·0345	30·358	74·567	138·59	222·45
	7	6·0345	30·358	74·566	138·59	222·42
	8	6·0345	30·358	74·565	138·58	222·41
1·0	1	6·3868				
	2	6·3814	29·735			
	3	6·3808	29·675	73·620		
	4	6·3807	29·664	73·514	137·42	
	5	6·3807	29·662	73·488	137·28	221·06
	6	6·3807	29·661	73·480	137·24	220·90
	7	6·3807	29·660	73·477	137·23	220·85
	8	6·3807	29·660	73·475	137·22	220·83
$n = 1$						
0·2	1	15·436				
	2	15·428	49·797			
	3	15·427	49·771	103·94		
	4	15·427	49·767	103·90	177·88	
	5	15·427	49·765	103·89	177·83	271·63
	6	15·427	49·765	103·89	177·82	271·58
	7	15·427	49·764	103·89	177·82	271·56
	8	15·427	49·764	103·89	177·81	271·55
1·0	1	14·960				
	2	14·943	48·804			
	3	14·941	48·745	102·63		
	4	14·940	48·733	102·53	176·33	
	5	14·940	48·729	102·51	176·21	269·85
	6	14·940	48·728	102·50	176·17	269·71
	7	14·940	48·727	102·50	176·16	269·66
	8	14·940	48·727	102·50	176·15	269·65

In Tables 3 and 4, the effect of free-surface waves on the nondimensional eigenfrequencies of the first three bulging and sloshing modes is investigated. It is assumed that the liquid–plate density ratio $\sigma = 0{\cdot}28$ and the plate thickness–radius ratio $\gamma = 0{\cdot}05$. Two different plate–container radius ratios, $\alpha = 0{\cdot}1$ and 1, two different liquid depth–radius ratios, $\beta = 0{\cdot}1$ and 1, and five different rigidity–gravity ratios, $t = 0{\cdot}1$, 1, 10, 100, 1000, are considered. In the present computations, $M = 40$, $I = 8$ and $J = 5$ are used. The results obtained when neglecting the interaction of bulging modes and sloshing modes are also given for comparison. One can see that the effect of free-surface waves on eigenfrequencies decreases with decreasing plate–container radius ratio α and increases with decreasing rigidity–gravity ratio t. However, the effect is significant only for the fundamental eigenfrequencies of axisymmetric modes ($n = 0$) under the small rigidity–gravity ratio condition ($t = 1$ and $0{\cdot}1$). From the above analysis we can conclude that in most cases, the interaction of bulging modes and sloshing modes can be neglected, unless the plates are extremely flexible.

TABLE 2
Nondimensional eigenfrequencies of bulging modes of clamped circular plates in contact with liquid by using different numbers of terms of the summing series; $I = 8$ and $J = 5$

α	m	λ_{1n}	λ_{2n}	λ_{3n}	λ_{4n}	λ_{5n}
$n = 0$						
0·2	5	6·1160	36·536	86·004	155·10	243·93
	10	6·0353	31·059	84·611	154·03	242·96
	20	6·0345	30·360	74·628	141·37	240·76
	30	6·0345	30·358	74·568	138·61	222·62
	40	6·0345	30·358	74·565	138·58	222·41
0·5	5	6·1322	30·357	78·365	152·97	242·21
	10	6·1322	30·342	74·530	138·62	223·72
	20	6·1322	30·341	74·520	138·52	222·33
	30	6·1322	30·341	74·520	138·52	222·33
	40	6·1322	30·341	74·520	138·52	222·33
1·0	5	6·1761	29·660	73·477	137·25	221·14
	10	6·1761	29·660	73·475	137·22	220·83
	20	6·1761	29·660	73·475	137·22	220·83
	30	6·1761	29·660	73·475	137·22	220·83
	40	6·1761	29·660	73·475	137·22	220·83
$n = 1$						
0·2	5	17·610	58·353	117·74	196·77	295·51
	10	15·464	55·222	116·39	195·62	294·43
	20	15·427	49·780	104·22	190·61	292·47
	30	15·427	49·765	103·90	177·89	272·32
	40	15·426	49·764	103·89	177·81	271·55
0·5	5	15·391	50·849	116·12	195·36	294·16
	10	15·385	49·693	103·83	177·98	287·05
	20	15·384	49·690	103·80	177·71	271·41
	30	15·384	49·690	103·80	177·71	271·40
	40	15·384	49·690	103·80	177·71	271·40
1·0	5	14·940	48·728	102·51	176·39	283·26
	10	14·940	48·727	102·50	176·15	269·65
	20	14·940	48·727	102·50	176·15	269·65
	30	14·940	48·727	102·50	176·15	269·65
	40	14·940	48·727	102·50	176·15	269·65

6. NUMERICAL RESULTS

In this section, some important results are reported from equation (51) when neglecting the effect of free-surface waves. In the computations, unless otherwise stated, the following parameters are used: the liquid–plate density ratio $\sigma = 0{\cdot}15$; the thickness–radius ratio of the plate $\gamma = 0{\cdot}05$: Poisson's ratio $\nu = 0{\cdot}3$. The numbers of terms used in the expansions of plate deflection and velocity potential are $M = 40$, $I = 8$ and $J = 5$.

Figure 2 gives the first six eigenfrequency ratios for the axisymmetric vibration ($n = 0$) of clamped circular plates with respect to α when $\beta = 1$. In the figure, r_i denotes (ith eigenfrequency of wet modes)/(ith eigenfrequency of dry modes). It is seen that, for a given circular plate, the eigenfrequencies converge rapidly to constant values as the radius of the container and the depth of the liquid increase. This implies that the liquid in a half-space can be approximately replaced by a liquid with larger radius and depth in the computation.

TABLE 3
The effect of free-surface waves on the nondimensional eigenfrequencies of bulging modes of clamped circular plates; only the first three modes for $n = 0$, 1 are reported

t	λ_{10}	λ_{20}	λ_{30}	λ_{11}	λ_{21}	λ_{31}
$\alpha = 1$, $\beta = 0{\cdot}1$						
0·1	8·4171	32·437	73·939	17·270	49·990	100·60
1	8·2320	32·398	73·927	17·188	49·969	100·59
10	8·2135	32·394	73·926	17·180	49·966	100·59
100	8·2116	32·394	73·935	17·179	49·966	100·59
1000	8·2114	32·394	73·935	17·179	49·966	100·59
	(8·2114)	(32·394)	(73·935)	(17·179)	(49·966)	(100·59)
$\alpha = 1$, $\beta = 1$						
0·1	5·3578	25·454	65·603	12·462	42·754	92·680
1	4·7891	25·434	65·601	12·426	42·754	92·680
10	4·7278	25·432	65·600	12·423	42·754	92·680
100	4·7217	25·432	65·600	12·422	42·754	92·680
1000	4·7211	25·432	65·600	12·422	42·754	92·680
	(4·7210)	(25·432)	(65·600)	(12·422)	(42·754)	(92·680)
$\alpha = 0{\cdot}1$, $\beta = 1$						
0·1	4·8059	26·191	66·817	12·989	43·967	94·344
1	4·7460	26·189	66·816	12·989	43·967	94·344
10	4·7397	26·188	66·816	12·989	43·967	94·344
100	4·7391	26·188	66·816	12·989	43·967	94·344
1000	4·7390	26·188	66·816	12·989	43·967	94·344
	(4·7390)*	(26·188)	(66·816)	(12·989)	(43·967)	(94·344)

* Data in parentheses are those when the effect of free-surface waves is neglected.

Figure 3 gives the first six eigenfrequency ratios for the axisymmetric vibration of clamped circular plates with respect to the plate–container radius ratio α. The depth–radius ratio of liquid is taken as $\beta = \alpha$, which means that the depth of the liquid is the same as the radius of the plate. It can be seen that the eigenfrequencies, especially the fundamental frequency, tend to become lower as α approaches unity ($\alpha = 1$ means that the bottom of the container is completely elastic). Moreover, one can find that for a given circular plate, the eigenfrequencies also converge rapidly to constant values with increasing radius of the container. This means that the liquid with infinite radius can be approximately replaced by a finite but larger-radius liquid in the computation.

Figure 4 gives the first six eigenfrequency ratios for the axisymmetric vibration of clamped circular plates with respect to the liquid depth–radius ratio β when the plate–container radius ratio $\alpha = 0{\cdot}5$. It is found that an increase of the liquid depth results in a decrease of the eigenfrequencies, and that the effect of the liquid depth on the fundamental mode is significantly larger than that on higher modes.

Figure 5 gives the first six eigenfrequency ratios for the axisymmetric vibration of clamped circular plates with respect to the density–thickness correction factor μ when the plate–container radius ratio $\alpha = 0{\cdot}5$ and the depth–radius ratio of liquid $\beta = 1$. One can see that eigenfrequencies decrease monotonically with increasing density–thickness correction factor μ.

Table 5 gives the first six nondimensional wet-mode eigenfrequencies of circular plates with elastically rotational constraint and zero deflection along the edge for the axisymmetric modes ($n = 0$) and the modes with a nodal diameter ($n = 1$). Two different plate–container radius ratios $\alpha = 1$ and 0·5, two different liquid depth–radius ratios, $\beta = 1$

TABLE 4
The effect of free-surface waves on the nondimensional eigenfrequencies of sloshing modes of liquids for clamped circular plates

t	λ_{10}	λ_{20}	λ_{30}	λ_{11}	λ_{21}	λ_{31}
$\alpha = 1$, $\beta = 0{\cdot}1$						
0·1	1·1703	2·0593	2·7963	0·057727	1·6084	2·4315
1	0·37379	0·65164	0·88437	0·18303	0·50983	0·76909
10	0·11832	0·20608	0·27966	0·057896	0·16126	0·24321
100	0·037421	0·065168	0·088438	0·018309	0·050996	0·076911
1 000	0·011834	0·020608	0·027966	0·0057898	0·016126	0·024321
$\alpha = 0$*, $\beta = 0{\cdot}1$						
0·1	1·1834	2·0608	2·7966	0·057898	1·6126	2·4321
1	0·37421	0·65168	0·88438	0·18309	0·50996	0·76911
10	0·11834	0·20608	0·27966	0·057898	0·16126	0·24321
100	0·037421	0·065168	0·088438	0·018309	0·050996	0·076911
1 000	0·011834	0·020608	0·027966	0·0057898	0·016126	0·024321
$\alpha = 1$, $\beta = 1$						
0·1	6·1904	8·3759	10·086	4·1705	7·3015	9·2392
1	1·9565	2·6487	3·1896	1·3228	2·3089	2·9217
10	0·61872	0·83759	1·0086	0·41841	0·73015	0·92392
100	0·19566	0·26487	0·31896	0·13232	0·23089	0·29217
1 000	0·061872	0·083759	0·10086	0·041843	0·073015	0·092392
$\alpha = 0{\cdot}1$, $\beta = 1$						
0·1	6·1887	8·3759	10·086	4·1842	7·3015	9·2392
1	1·9565	2·6487	3·1896	1·3232	2·3089	2·9217
10	0·61872	0·83759	1·0086	0·41843	0·73015	0·92392
100	0·19566	0·26487	0·31896	0·13232	0·23089	0·29217
1 000	0·061872	0·083759	0·10086	0·041843	0·073015	0·092392
$\alpha = 0$*, $\beta = 1$						
0·1	6·1872	8·3759	10·086	4·1843	7·3015	9·2392
1	1·9566	2·6487	3·1896	1·3232	2·3089	2·9217
10	0·61872	0·83759	1·0086	0·41843	0·73015	0·92392
100	0·19566	0·26487	0·31896	0·13232	0·23089	0·29217
1 000	0·061872	0·083759	0·10086	0·041843	0·073015	0·092392

* Completely rigid bottom.

and 0·5, and three different nondimensional rotational stiffnesses, $K_\psi = 1$, 10 and 100, are considered. It can be seen that the eigenfrequencies increase with the increase of the stiffness of the rotational constraint.

7. NAVMI FACTOR SOLUTION

From equation (51) one can find that, if the NAVMI matrix $[\bar{M}]$ is a diagonal one, the analysis will be greatly simplified. In this case, the wet-mode parameters can be directly given as $\lambda_{in} = k_{in}^2/\sqrt{1 + \mu \bar{M}_{ii}^n}$, in which $\bar{M}_{ii}^n$ is the ith diagonal element of $[\bar{M}]$ corresponding to the nth nodal diameter and is called the NAVMI factor (Kwak 1991); this means that the wet modes of the plate are the same as those of the dry modes. This simplification has an obvious advantage, in that the NAVMI factors, being independent of the density–thickness correction factor μ, need only to be computed once and can be used for all cases. Unfortunately, in fact, the matrix $[\bar{M}]$ is never a diagonal one, although it is a diagonally

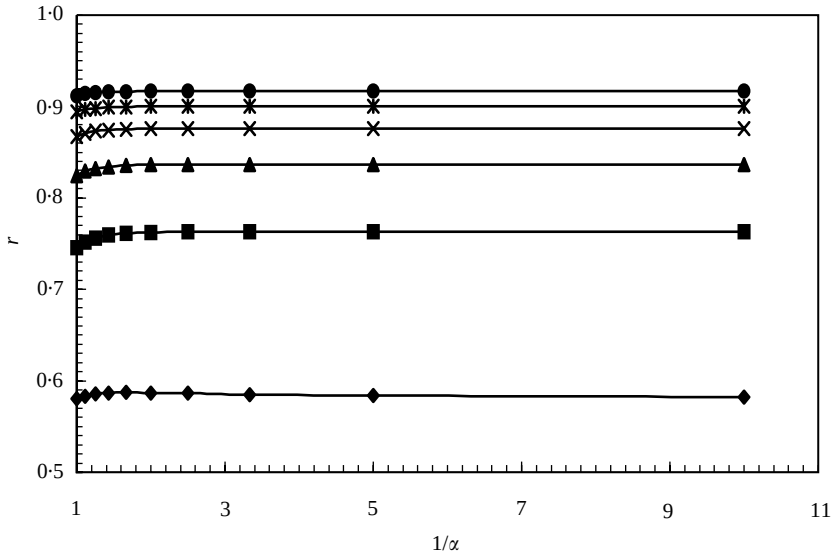

Figure 2. The first six eigenfrequency ratios r_i ($i = 1, 2, \ldots, 6$) of wet modes and dry modes for axisymmetric vibration ($n = 0$) of clamped circular plates as a function of the plate–container radius ratio α; $\beta = 1$. ◆, r_1; ■, r_2; ▲, r_3; ×, r_4; ✳, r_5; ●, r_6.

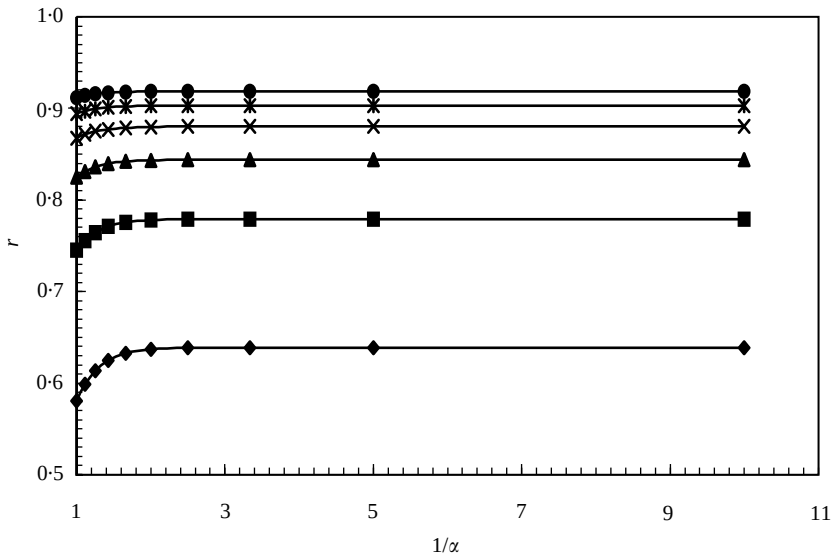

Figure 3. The first six eigenfrequency ratios r_i ($i = 1, 2, \ldots, 6$) of wet modes and dry modes for axisymmetric vibration ($n = 0$) of clamped circular plates as a function of the plate–container radius ratio α; $\beta = \alpha$. ◆, r_1; ■, r_2; ▲, r_3; ×, r_4; ✳, r_5; ●, r_6.

dominant matrix in many cases. Therefore, it is of great importance to know the extent of error in NAVMI factor solutions used in engineering problems.

The percentage error in the NAVMI factor solution versus the Galerkin solution for a clamped circular plate is given in Figure 6 with respect to the density–thickness correction factor μ for $\beta = 1$ and $\alpha = 0{\cdot}5$. The first three axisymmetric modes ($n = 0$) and the first two

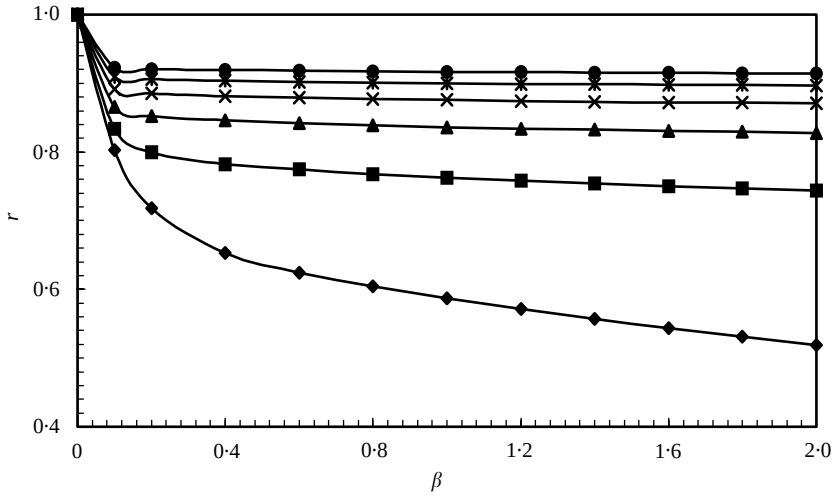

Figure 4. The first six eigenfrequency ratios r_i ($i = 1, 2, \ldots, 6$) of wet modes and dry modes for the axisymmetric vibration ($n = 0$) of clamped circular plates as a function of the depth–radius ratio of liquid β; $\alpha = 0{\cdot}5$. ◆, r_1; ■, r_2; ▲, r_3; ×, r_4; ✳, r_5; ●, r_6.

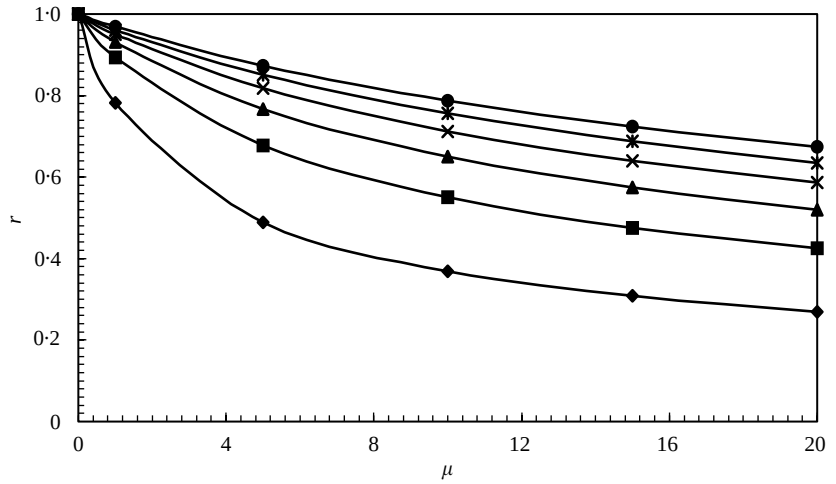

Figure 5. The first six eigenfrequency ratios r_i ($i = 1, 2, \ldots, 6$) of wet modes and dry modes for the axisymmetric vibration ($n = 0$) of clamped circular plates as a function of the density–thickness correction factor μ; $\alpha = 0{\cdot}5$ and $\beta = 1$. ◆, r_1; ■, r_2; ▲, r_3; ×, r_4; ✳, r_5; ●, r_6.

modes with one and two nodal diameters ($n = 1, 2$) are investigated. In the figure, e denotes $(1 - 2\ NAVMI\ factor\ solution/Galerkin\ solution) \times 100$. Figure 7 gives the percentage error with respect to β when $\mu = 10$, $\alpha = 0{\cdot}5$ and Figure 8 gives those with respect to α when $\mu = 10$, $\beta = \alpha$. From Figures 6 and 7, one can see that both the density–thickness correction factor μ and the liquid depth–radius ratio β have a larger effect on the error in NAVMI factor solutions for the axisymmetric modes with nodal circles ($i \geq 2$), and the errors increase with μ and β. However, the effect of μ and β on the error in NAVMI factor solutions for other wet modes, especially for wet modes without nodal circles ($i = 1$) is very

TABLE 5
Nondimensional eigenfrequencies of the first six bulging modes of circular plates with elastically rotational constraints and zero deflection along the edge

β	K_ψ	α	λ_{1n}	λ_{2n}	λ_{3n}	λ_{4n}	λ_{5n}	λ_{6n}
$n = 0$								
1	1	1	3·3368	22·837	62·202	121·36	200·30	299·01
		0·5	3·4142	23·464	63·087	122·42	201·50	300·32
	10	1	4·9548	26·004	66·373	126·23	205·69	304·79
		0·5	5·0372	26·716	67·407	127·475	207·08	306·30
	100	1	5·7911	29·011	72·019	134·65	216·87	318·66
		0·5	5·8629	29·713	73·087	135·98	218·41	320·37
0·5	1	1	4·0338	23·561	62·771	121·87	200·77	299·46
		0·5	3·7610	23·845	63·474	122·81	201·88	300·70
	10	1	5·9017	27·029	67·206	126·95	206·34	305·39
		0·5	5·5040	27·249	67·939	127·99	207·59	306·80
	100	1	6·8220	30·205	73·090	135·63	217·79	319·54
		0·5	6·3687	30·320	73·727	136·64	219·07	321·04
$n = 1$								
1	1	1	10·093	39·460	88·681	157·70	246·51	355·08
		0·5	10·567	40·322	89·771	158·96	247·90	356·58
	10	1	12·739	43·342	93·370	162·97	252·20	361·12
		0·5	13·238	44·332	94·647	164·44	253·82	362·85
	100	1	14·581	47·720	100·51	172·91	264·88	376·44
		0·5	15·054	48·707	101·85	174·51	266·70	378·43
0·5	1	1	10·696	39·870	89·008	158·00	246·78	355·34
		0·5	10·687	40·442	89·892	159·08	248·02	356·70
	10	1	13·424	43·904	93·833	163·37	252·57	361·46
		0·5	13·370	44·484	94·804	164·60	253·98	363·00
	100	1	15·283	48·378	101·11	173·46	265·41	376·95
		0·5	15·185	48·872	102·03	174·70	266·90	378·63

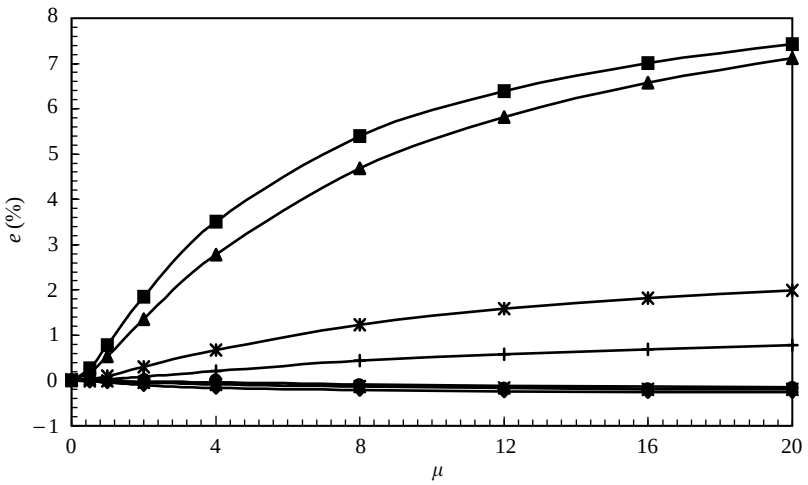

Figure 6. The percentage error in the eigenfrequencies obtained via NAVMI factor solution versus the Galerkin solution for clamped circular plates in contact with liquid as a function of the density–thickness correction factor μ; $\beta = 1$ and $\alpha = 0{\cdot}5$. ◆, $n = 0, i = 1$; ■, $n = 0, i = 2$; ▲, $n = 0, i = 3$; ×, $n = 1, i = 1$; ✳, $n = 1, i = 2$; ●, $n = 1, i = 3$.

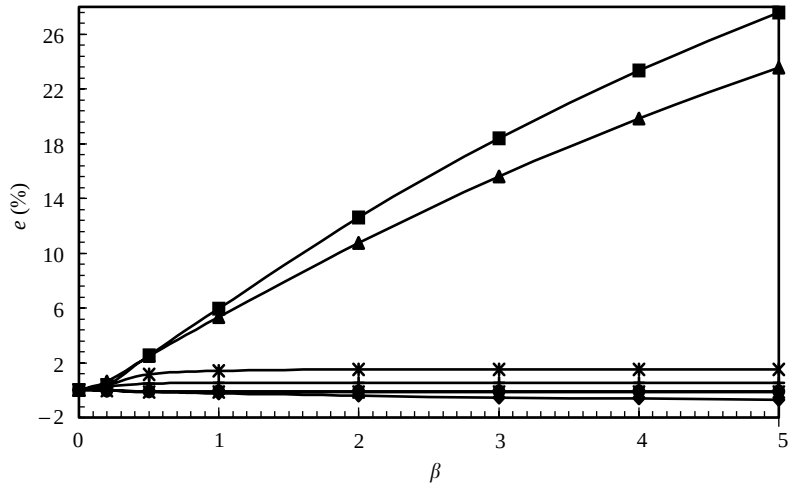

Figure 7. The percentage error in the eigenfrequencies obtained via NAVMI factor solution versus the Galerkin solution for clamped circular plates in contact with liquid as a function of the depth–radius ratio of the liquid β; $\mu = 10$ and $\alpha = 0{\cdot}5$. ◆, $n = 0$, $i = 1$; ■, $n = 0$, $i = 2$; ▲, $n = 0$, $i = 3$; ×, $n = 1$, $i = 1$; ✳, $i = 2$; ●, $n = 1$, $i = 3$.

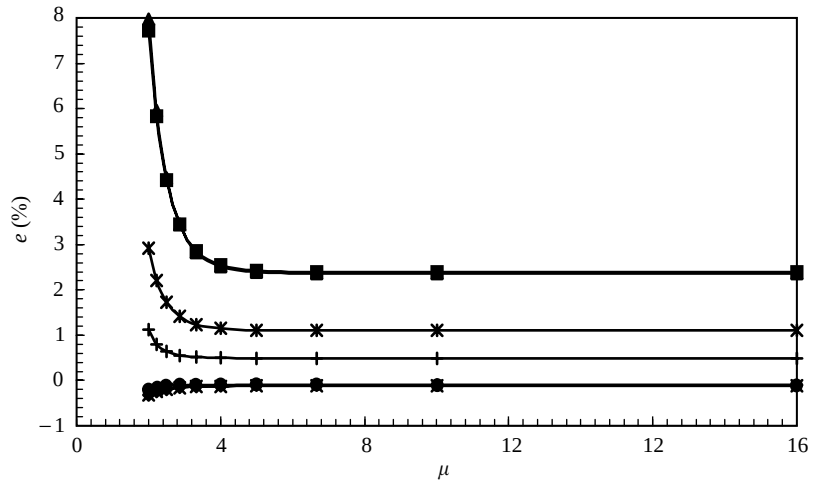

Figure 8. The percentage error in the eigenfrequencies obtained via NAVMI factor solution versus the Galerkin solution for clamped circular plates in contact with liquid as a function of the plate–container radius ratio α; $\mu = 10$ and $\beta = \alpha$. ◆, r_1; ■, r_2; ▲, r_3; ×, r_4; ✳, r_5; ●, r_6.

small. Moreover, from Figure 8, it is seen that the maximum error in the NAVMI factor solutions occurs for $\alpha = 1$ (in this case, the bottom of the container is completely elastic). However, the error quickly decreases and reaches a plateau as the container radius is increased.

The NAVMI factors for circular plates with elastically rotational constraints and zero deflection along the edge have been studied in detail. Three NAVMI factors for axisymmetric modes ($n = 0$), two NAVMI factors for the modes with one nodal diameter ($n = 1$) and one NAVMI factor for the modes with two nodal diameters ($n = 2$) are given in Tables 6 and 7, respectively. Seven different plate–container radius ratios, $\alpha = 1$, 0·9, 0·8, 0·7, 0·6, 0·5 and 0·1, and two different liquid depth–radius ratios, $\beta = 1$ and $\beta = \alpha$, are considered. The

TABLE 6
NAVMI factors $\tilde{M}_{ii}^{n}$ for circular plates with elastically rotational constraint and zero deflection on edge; axisymmetric modes ($n = 0$)

K_ψ	i	$\alpha = 1$	$\alpha = 0{\cdot}9$	$\alpha = 0{\cdot}8$	$\alpha = 0{\cdot}7$	$\alpha = 0{\cdot}6$	$\alpha = 0{\cdot}5$	$\alpha = 0{\cdot}1$	$\alpha = 0$
$\beta = 1$									
0	1	0·78213	0·75929	0·74400	0·73454	0·72974	0·72869	0·74780	(0·75539)*
	2	0·30529	0·28580	0·27314	0·26475	0·25934	0·25610	0·25553	(0·25680)
	3	0·17607	0·16493	0·15846	0·15438	0·15182	0·15031	0·14988	(0·15041)
1	1	0·76529	0·74436	0·73038	0·72181	0·71757	0·71683	0·73566	(0·743)
	2	0·31312	0·29308	0·27997	0·27126	0·26564	0·26231	0·26200	(0·264)
	3	0·17964	0·16807	0·16129	0·15700	0·15430	0·15270	0·15231	
10	1	0·70301	0·68827	0·67856	0·67287	0·67043	0·67065	0·68826	(0·694)
	2	0·32864	0·30900	0·29583	0·28701	0·28134	0·27806	0·27882	(0·281)
	3	0·19323	0·18051	0·17273	0·16773	0·16457	0·16271	0·16252	
100	1	0·66060	0·64946	0·64224	0·63821	0·63681	0·63756	0·65418	(0·661)
	2	0·31841	0·30182	0·29048	0·28284	0·27796	0·27518	0·27660	(0·278)
	3	0·19402	0·18239	0·17499	0·17016	0·16710	0·16531	0·16541	
∞	1	0·65320	0·64264	0·63583	0·63207	0·63084	0·63167	0·64810	(0·65381)
	2	0·31406	0·29827	0·28744	0·28014	0·27547	0·27284	0·27434	(0·27613)
	3	0·19151	0·18048	0·17341	0·16877	0·16583	0·16412	0·16428	(0·16513)
$\beta = \alpha$									
0	1	0·78213	0·69537	0·63000	0·58374	0·55425	0·53842	0·53059	[0·53059]†
	2	0·30529	0·27482	0·25365	0·23925	0·23023	0·22541	0·22304	[0·22304]
	3	0·17607	0·16040	0·15041	0·14384	0·13978	0·13763	0·13656	[0·13656]
1	1	0·76529	0·68255	0·62012	0·57592	0·54773	0·53260	0·52512	
	2	0·31312	0·28086	0·25828	0·24287	0·23319	0·22803	0·22548	
	3	0·17964	0·16314	0·15251	0·14550	0·14116	0·13886	0·13772	
10	1	0·70301	0·63419	0·58202	0·54501	0·52138	0·50870	0·50242	
	2	0·32864	0·29359	0·26846	0·25112	0·24019	0·23435	0·23146	
	3	0·19323	0·17386	0·16092	0·15225	0·14685	0·14398	0·14256	
100	1	0·66060	0·60058	0·55496	0·52254	0·50183	0·49071	0·48521	
	2	0·31841	0·28633	0·26297	0·24674	0·23647	0·23098	0·22826	
	3	0·19402	0·17507	0·16199	0·15311	0·14755	0·14459	0·14312	
∞	1	0·65320	0·59467	0·55015	0·51852	0·49830	0·48745	0·48208	
	2	0·31406	0·28303	0·26037	0·24460	0·23463	0·22929	0·22665	
	3	0·19151	0·17325	0·16056	0·15192	0·14650	0·14362	0·14219	

* The values in ( ) are from Amabili & Kwak (1996).
† The values in [ ] are from Amabili (1996).

available results from literature for the limiting cases (infinite radius liquid) are also given for comparison (Amabili and Kwak 1996; Amabili 1996).

It is seen that all the NAVMI solutions are close to the limiting cases as the container radius is increased. This demonstrates once again that, using the present method, the infinite liquid can be replaced by finite but larger-size liquid in the computation without serious error.

8. CONCLUSIONS

The theoretical solution for the hydroelastic vibration of circular plates is presented. The plate is placed into a hole of the rigid bottom slab of a circular cylindrical container

TABLE 7
NAVMI factors $\tilde{M}_{ii}^{n}$ for circular plates with elastically rotational constraint and zero deflection on edge; the modes with one and two nodal diameters ($n = 1, 2$)

K_ψ	n,i	$\alpha = 1$	$\alpha = 0{\cdot}9$	$\alpha = 0{\cdot}8$	$\alpha = 0{\cdot}7$	$\alpha = 0{\cdot}6$	$\alpha = 0{\cdot}5$	$\alpha = 0{\cdot}1$	$\alpha = 0$
$\beta = 1$									
0	1,1	0·40489	0·37993	0·36296	0·35134	0·34352	0·33842	0·33221	(0·33225)*
	1,2	0·20036	0·18776	0·18046	0·17595	0·17313	0·17141	0·16952	(0·16951)
	2,1	0·26173	0·24520	0·23629	0·23143	0·22884	0·22753	0·22675	(0·22675)
1	1,1	0·39866	0·37493	0·35873	0·34762	0·34012	0·33522	0·32933	(0·329)
	1,2	0·20246	0·18955	0·18198	0·17729	0·17435	0·17254	0·17055	
	2,1	0·25898	0·24318	0·23464	0·22996	0·22747	0·22620	0·22545	(0·225)
10	1,1	0·37107	0·35231	0·33929	0·33026	0·32412	0·32009	0·31519	(0·315)
	1,2	0·20681	0·19374	0·18577	0·18072	0·17750	0·17551	0·17326	
	2,1	0·24536	0·23285	0·22599	0·22220	0·22015	0·21910	0·21848	(0·219)
100	1,1	0·34683	0·33194	0·32143	0·31408	0·30904	0·30571	0·30163	(0·301)
	1,2	0·20031	0·18911	0·18204	0·17746	0·17451	0·17266	0·17055	
	2,1	0·23089	0·22142	0·21615	0·21320	0·21158	0·21073	0·21024	(0·210)
∞	1,1	0·34208	0·32789	0·31786	0·31082	0·30598	0·30278	0·29886	(0·29883)
	1,2	0·19750	0·18690	0·18017	0·17578	0·17295	0·17117	0·16914	(0·16914)
	2,1	0·22774	0·21888	0·21393	0·2115	0·20962	0·20881	0·20835	(0·20834)
$\beta = \alpha$									
0	1,1	0·40489	0·37391	0·35201	0·33708	0·32781	0·32299	0·32071	[0·32071]†
	1,2	0·20036	0·18653	0·17806	0·17266	0·16941	0·16774	0·16695	[0·16695]
	2,1	0·26173	0·24465	0·23528	0·23011	0·22743	0·22620	0·22575	
1	1,1	0·39866	0·36910	0·34824	0·33396	0·32504	0·32032	0·31812	
	1,2	0·20246	0·18822	0·17949	0·17392	0·17046	0·16863	0·16780	
	2,1	0·25898	0·24264	0·23365	0·22868	0·22610	0·22492	0·22449	
10	1,1	0·37107	0·34729	0·33032	0·31863	0·31129	0·30739	0·30559	
	1,2	0·20681	0·19213	0·18277	0·17670	0·17290	0·17090	0·16999	
	2,1	0·24536	0·23238	0·22514	0·22111	0·21899	0·21801	0·21766	
100	1,1	0·34683	0·32762	0·31376	0·30416	0·29811	0·29488	0·29339	
	1,2	0·20031	0·18750	0·17907	0·17351	0·17002	0·16817	0·16732	
	2,1	0·23089	0·22103	0·21545	0·21231	0·21063	0·20984	0·20956	
∞	1,1	0·34208	0·32371	0·31043	0·30123	0·29542	0·29231	0·29089	
	1,2	0·19750	0·18533	0·17727	0·17195	0·16859	0·16681	0·16599	
	2,1	0·22774	0·21851	0·21326	0·21030	0·20871	0·20796	0·20770	

* The values in ( ) are from Amabili & Kwak (1996).
† The values in [ ] are from Amabili (1996).

partially filled with liquid. The exact solution for the velocity potential of liquid motions is given by the method of separation of variables. Part of the unknown coefficients in the potential velocity is determined by using the Fourier–Bessel expansion to the liquid–plate interface equation, in the form of integrals associated with the dynamic deflection of the plate. The Galerkin method is applied to derive the eigenfrequency equation from the governing equation of plate vibration under the hydrodynamic pressure and the equation of free-surface waves. The high accuracy and small computational cost are demonstrated by the convergence study. The effect of free-surface waves on eigenfrequencies of both bulging and sloshing modes is studied. It is shown that, in most cases, the interaction between bulging modes and sloshing modes can be neglected, unless the plates are extremely flexible.

The effects of size and density parameters of both the plate and the liquid on the bulging modes of liquid–plate interaction are discussed in detail. As a consequence, the NAVMI

factor solution is also given and its accuracy is evaluated by comparing with the more accurate Galerkin solution. Moreover, the results show that for a given circular plate, eigenfrequencies tend to converge to constant values with increasing radius of the container. This means that the present method is also applicable to study the hydroelastic vibrations of circular plates in contact with infinite liquid, by considering a finite but larger-size liquid to replace the infinite liquid in the computation.

References

Amabili, M. 1996 Effect of finite fluid depth on the hydroelastic vibrations of circular and annular plates. *Journal of Sound and Vibration* **193**, 909–925.

Amabili, M. 1997 Bulging modes of circular bottom plates in rigid cylindrical containers filled with a liquid. *Shock and Vibration* **4**, 51–68.

Amabili, M. 2000 Eigenvalue problems for vibrating structures coupled with quiescent fluids with free surface. *Journal of Sound and Vibration* **231**, 79–97.

Amabili, M. & Dalpiaz, G. 1998 Vibrations of base plates in annular cylindrical containers: theory and experiments. *Journal of Sound and Vibration* **210**, 329–350.

Amabili, M. & Kwak, M. K. 1996 Free vibrations of circular plates coupled with liquids: revising the Lamb problem. *Journal of Fluids and Structures* **10**, 743–761.

Amabili, M. & Kwak, M. K. 1999 Vibration of circular plates on a free fluid surface: effect of surface waves. *Journal of Sound and Vibration* **226**, 407–424.

Amabili, M., Païdoussis, M. P. & Lakis, A. A. 1998 Vibrations of partially filled cylindrical tanks with ring-stiffeners and flexible bottom. *Journal of Sound and Vibration* **213**, 259–299.

Bauer, H. F. 1981 Hydroelastic vibrations in a rectangular container. *International Journal of Solids and Structures* **17**, 639–652.

Bauer, H. F. 1995 Coupled frequencies of a liquid in a circular cylindrical container with elastic liquid surface cover. *Journal of Sound and Vibration* **180**, 689–704.

Bauer, H. F., Chang, S. S. & Wang, J. T. S. 1971 Nonlinear liquid motion in a longitudinally excited container with elastic bottom. *AIAA Journal* **9**, 2333–2339.

Bhuta, P. G. & Koval, L. R. 1964*a* Coupled oscillations of a liquid with a free surface in a container having a flexible bottom. *Zeitschrift für Angewandte Mathematik und Physik* **15**, 466–480.

Bhuta, P. G. & Koval, L. R. 1964*b* Hydroelastic solution of the sloshing of a liquid in a cylindrical container. *Journal of the Acoustical Society of America* **36**, 2071–2079.

Cheung, Y. K. & Zhou, D. 2000 Coupled vibratory characteristics of a rectangular container bottom plate. *Journal of Fluids and Structures* **14**, 339–357.

Chiba, M. 1993 Nonlinear hydroelastic vibration of a cylindrical container with an elastic bottom, containing liquid. Part II: linear axisymmetric vibration analysis. *Journal of Fluids and Structures* **7**, 57–73.

Chiba, M. 1994 Axisymmetric free hydroelastic vibration of a flexural bottom plate in a cylindrical container supported on an elastic foundation. *Journal of Sound and Vibration* **169**, 387–394.

Espinosa, F. M. & Gallego-Juarez, J. A. 1984 On the resonance frequencies of water-loaded circular plates. *Journal of Sound and Vibration* **94**, 217–222.

Kwak, M. K. 1991 Vibration of circular plates in contact with water. *Journal of Applied Mechanics* **58**, 480–483.

Kwak, M. K. 1997 Hydroelastic vibration of circular plates. *Journal of Sound and Vibration* **201**, 293–303.

Lamb, H. 1921 On the vibrations of an elastic plate in contact with water. *Proceedings of the Royal Society of London*, Series A **98**, 205–216.

Leissa, A. W. 1969 Vibration of plates. NASA SP-160, Government Printing Office, Washington, DC, U.S.A.

McLachlan, N. W. 1961 *Bessel Functions for Engineers*. Amen House, London: Oxford University Press.

Morand, H. J.-P. & Ohayon, R. 1995 *Fluid Structure Interaction: Applied Numerical Methods*. Chichester: John Wiley.

Tong, P. 1967 Liquid motion in a circular cylindrical container with a flexible bottom. *AIAA Journal* **5**, 1842–1848.

Tsui, T. Y. & Small, N. C. 1968 Hydroelastic oscillations of a liquid surface in an annular circular cylindrical container with flexible bottom. *Journal of Spacecraft and Rockets* **5**, 202–206.

Zhou, D. & Cheung, Y. K. 2000 Vibration of vertical rectangular plate in contact with water on one side. *Earthquake Engineering and Structural Dynamics* **29**, 693–710.